

**Quenching of spontaneous emission through interference of incoherent pump processes**Kishore T. Kapale,<sup>1</sup> Marlan O. Scully,<sup>1,2</sup> Shi-Yao Zhu,<sup>1,3</sup> and M. Suhail Zubairy<sup>1,4</sup><sup>1</sup>*Institute for Quantum Studies and Department of Physics, Texas A & M University, College Station, Texas 77843-4242*<sup>2</sup>*Max-Planck-Institut für Quantenoptik, D-85748 Garching, Germany*<sup>3</sup>*Department of Physics, Hong Kong Baptist University, Hong Kong, China*<sup>4</sup>*Department of Electronics, Quaid-i-Azam University, Islamabad, Pakistan*

(Received 9 July 2002; revised manuscript received 14 October 2002; published 7 February 2003)

We investigate the steady-state spontaneous emission of a V-type three-level atom, with the coherence between the two upper levels modified and controlled via incoherent pumping to a fourth auxiliary level. The external pumping gives us an easily controllable handle in manipulating the spontaneous emission to such an extent that, under certain conditions, complete quenching of spontaneous emission is possible. We also show that even the interference between the decay channels, which is considered a key requirement in spontaneous emission quenching through quantum interference, is not essential to achieve near 100% trapping and almost complete suppression of spontaneous emission. Thus we provide a scheme for spontaneous emission quenching which can be easily realized experimentally.

DOI: 10.1103/PhysRevA.67.023804

PACS number(s): 42.50.Ct, 42.50.Gy, 42.50.Lc

**I. INTRODUCTION**

Atomic coherence plays a crucial role in modifying spectral properties of a multilevel atomic system. The novel effects possible through generation of atomic coherence among atomic levels include correlated spontaneous emission laser [1], absorption cancellation (or lasing without inversion) [2–4], electromagnetically induced transparency [5], and spontaneous emission reduction and cancellation [4,6–8]. The generation of atomic coherence is usually achieved by application of strong coherent field tuned to an atomic transition of a multilevel atomic system [9] leading to coherently generated Autler-Townes doublet. Atomic coherence between two close lying levels can also be achieved through quantum interference of processes such as coupling of these levels to identical modes of a reservoir [6], or pumpings from them to a single upper lying atomic level [10]. Interfering spontaneous decay channels have also been shown to facilitate continuous wave lasing without inversion [11]. A nice review article appeared recently [12] that summarizes the quantum interference effects in optical fields and atomic radiation. The article also discusses the problem of control of spontaneous emission through quantum interference effects.

In the simplest scheme, spontaneous emission cancellation due to quantum interference of spontaneous transitions from two upper levels to a lower lying third level is possible only if the upper levels are closely spaced. The proximity of the levels is essential to ensure the existence of coherence and sufficient coupling between the two decaying channels. This limitation is overcome in Refs. [6,7] by introducing an auxiliary fourth level and coupling it to the two upper levels by a coherent field. Thus, spontaneous emission control is possible for arbitrarily spaced energy levels decaying to a common lower level by varying the parameters of the coherent field. In this setup, the auxiliary fourth level needs to be of lower energy than the doublet to maintain the quantum interference. We, however, wish to achieve even more control over the total spontaneous emission from the atom

through external parameters that can be manipulated with ease.

In this paper, we utilize interference of incoherent pump processes on the same lines as in Ref. [10], to introduce coherence between the decaying doublet. We insert an auxiliary level at an energy above the doublet and allow it to couple to the decaying doublet by interfering incoherent pump processes. These pump processes provide an extra handle on the fluorescence and a means of controlling the amount of coherent population trapping. Moreover, we maintain the advantage that the levels can be well separated by coupling the decaying doublet to the ground level through a coherent field. We observe that by controlling the parameters of the pumping fields, we can achieve further quenching of spontaneous emission than the simple case of interfering decay channels. We also observe that in certain range of values of the pumping parameters it is possible to have near 100% trapping in the decaying doublet, thus, achieving almost complete spontaneous emission quenching even in the absence of interference between the decay channels. To note, experimental work on quenching of spontaneous emission through quantum interference of two spontaneous decay channels has proved extremely difficult, with only one experiment so far [13], nevertheless, with criticism [14], due to the inherent uncontrollable nature of spontaneous emission processes. Our scheme suggests a possibility of achieving complete control over the total decay from a doublet through a very simple scheme which could be easily employed experimentally.

The article is organized as follows: In Sec. II, we discuss the essential ingredients of the model, discuss the Hamiltonian, and give the complete set of density-matrix equations for the atomic system. We provide a dressed-state picture of the model in Sec. III to allow for physical intuition of the results obtained by solving the density-matrix equation. In Sec. IV, we summarize various results obtained through the solution of density-matrix equations. We study the time dependent behavior of the populations of the atomic states and show the existence of coherent population trapping under

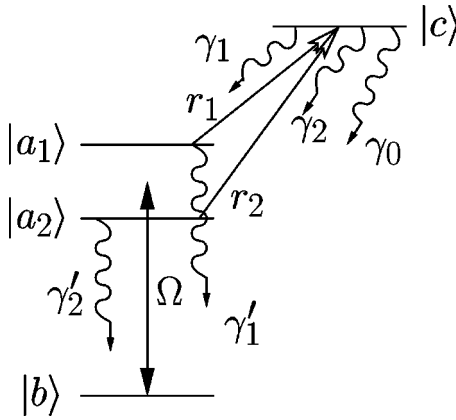


FIG. 1. The level scheme. We are interested in controlling the spontaneous emission from the doublet  $|a_1\rangle$  and  $|a_2\rangle$  to level  $|b\rangle$ . Level  $|c\rangle$  is the auxiliary level coupled to the doublet via incoherent pumpings  $r_1$  and  $r_2$ .

certain conditions. We also explore the effect of the energy spacing between two atomic levels on the coherence generated between them. Furthermore, we investigate the effect of quantum interference on the coherent population trapping and the spontaneous emission spectrum of the system. We review a similar model considered earlier in Ref. [7] in Sec. V and compare their results with our findings. In Sec. VI, we state our conclusions. Various calculational details such as the occurrence of quantum interference in the decay and the pump channels and the determination of spontaneous emission spectrum are considered in Appendixes A, B, and C.

## II. THE MODEL AND THE DENSITY-MATRIX EQUATIONS

We consider a level scheme depicted in Fig. 1. The spontaneous decay rates from  $|a_1\rangle$  and  $|a_2\rangle$  to  $|b\rangle$  are denoted by  $\gamma'_1$  and  $\gamma'_2$ , respectively. Incoherent pump processes  $r_1$  and  $r_2$  couple  $|a_1\rangle$  and  $|a_2\rangle$  to an auxiliary state  $|c\rangle$ . A coherent field is set to couple  $|b\rangle$  to both the states  $|a_1\rangle$  and  $|a_2\rangle$  by choosing a frequency tuned halfway between the two. We also include decays from state  $|c\rangle$  to all the lower levels.

There are three major dynamical processes occurring in the system: (i) interaction of the atomic system with the coherent field, (ii) incoherent pump processes through  $r_1$  and  $r_2$ , and (iii) interaction with the reservoir governing the decay processes from states  $|a_1\rangle$  and  $|a_2\rangle$  to the ground level. We describe these processes by interaction terms  $\mathcal{V}_1$ ,  $\mathcal{V}_2$ , and  $\mathcal{V}_3$ , respectively. Thus, including the free-energy terms, the total Hamiltonian is

$$\mathcal{H} = \mathcal{V}_0 + \mathcal{V}_1 + \mathcal{V}_2 + \mathcal{V}_3. \quad (1)$$

The detailed form of these terms in the Hamiltonian can be written as

$$\begin{aligned} \mathcal{V}_0 = & \hbar \omega_1 |b\rangle\langle b| + \hbar \omega_2 |a_2\rangle\langle a_2| + \hbar \omega_3 |a_1\rangle\langle a_1| \\ & + \hbar \omega_4 |c\rangle\langle c|, \end{aligned} \quad (2)$$

$$\mathcal{V}_1 = -\hbar \Omega_1 e^{-i\nu t} |a_1\rangle\langle b| - \hbar \Omega_2 e^{-i\nu t} |a_2\rangle\langle b| + \text{H.c.}, \quad (3)$$

$$\begin{aligned} \mathcal{V}_2 = & -\hbar \sum_k g_k^{(1)} e^{-i\nu_k t} |a_1\rangle\langle b| \hat{b}_k + g_k^{(2)} e^{-i\nu_k t} |a_2\rangle\langle b| \\ & \times \langle b| \hat{b}_k + \text{H.c.}, \end{aligned} \quad (4)$$

$$\mathcal{V}_3 = -p_1 \mathcal{E}_p |c\rangle\langle a_1| - p_2 \mathcal{E}_p |c\rangle\langle a_2| + \text{H.c.}, \quad (5)$$

where  $\Omega_1$  and  $\Omega_2$  are the Rabi frequencies of the coherent driving field of frequency  $\nu$  corresponding to the two transitions from  $|a_1\rangle$  and  $|a_2\rangle$  to  $|b\rangle$ , respectively;  $g_k^{(1,2)}$  are the coupling constants between the  $k$ th vacuum mode of frequency  $\nu_k$  and the atomic transition from  $|a_1\rangle$  and  $|a_2\rangle$  to  $|b\rangle$ , respectively, and  $p_1$  and  $p_2$  are the dipole moments of the atomic transitions corresponding to the pumpings from  $|a_1\rangle$  and  $|a_2\rangle$  to  $|c\rangle$ , respectively. To illustrate, the interaction term  $\mathcal{V}_2$  describes coupling of states  $|a_1\rangle$  and  $|a_2\rangle$  to state  $|b\rangle$  through identical vacuum modes. Thus, there is a possibility of quantum interference between the two decay modes. The interaction term  $\mathcal{V}_3$  describes coupling of states  $|a_1\rangle$  and  $|a_2\rangle$  to  $|c\rangle$  through a single electric field  $\mathcal{E}_p$ , which is taken to be complex to include the frequency dependent phase factor.

The dipole moments  $p_1$  and  $p_2$  corresponding to transitions from  $|a_1\rangle$  and  $|a_2\rangle$  to  $|c\rangle$  can, in principle, have different directions. However, the electric field  $\mathcal{E}_p$  can be chosen in a polarization mode such that it couples to both the transitions. Moreover, the electric field is required to have a broad frequency spectrum or effective  $\delta$ -like correlation, i.e.,

$$\langle \mathcal{E}_p^*(t) \mathcal{E}_p(t') \rangle = \Gamma_p \delta(t - t'). \quad (6)$$

The effect of  $\mathcal{V}_3$  can be summarized through the pumping parameters  $r_{1,2} = 2(p_{1,2}^2 / \hbar^2) \Gamma_p$  as discussed in Appendix B. We can treat the interaction terms separately to obtain the corresponding terms in the density-matrix equations to arrive at the final form. The effect of the interaction potentials, as well as the free part of the Hamiltonian  $\mathcal{V}_0$  on the density-matrix can be obtained using the Liouville equation

$$\begin{aligned} \dot{\rho}^{(0,1,2,3)} = & -\frac{i}{\hbar} [\mathcal{V}_{0,1,2,3}(t), \rho^{(0,1,2,3)}(t)] \\ = & -\frac{i}{\hbar} [\mathcal{V}_{0,1,2,3}(t) \rho^{(0,1,2,3)}(t) - \rho^{(0,1,2,3)}(t) \mathcal{V}_{0,1,2,3}(t)]. \end{aligned} \quad (7)$$

Here, the complete density-matrix has been reduced to different parts as

$$\rho = \rho^{(0)} + \rho^{(1)} + \rho^{(2)} + \rho^{(3)}, \quad (8)$$

coupling only to the corresponding part of the Hamiltonian. The terms corresponding to  $\mathcal{V}_0$  and  $\mathcal{V}_1$  can be obtained in a straightforward manner. However, calculation of the interference effect due to  $\mathcal{V}_2$  and  $\mathcal{V}_3$  is little more involved. We discuss the details of the appearance of decay and pump

interference terms in Appendixes A and B. Next we transform, thus, obtained equations to rotated frame and include all the atomic decays as shown in Fig. 1 through the usual procedure. A word of caution is necessary at this point, the

Hamiltonian does not explicitly include the decay terms and they are to be included in the density-matrix equation by following the usual procedure (see, for example, Ref. [15]). The resulting set of equations is

$$\begin{aligned}
 \dot{\tilde{\rho}}_{ba_2} &= \left[ -\frac{1}{2}(r_2 + \gamma'_2) + i\Delta_2 \right] \tilde{\rho}_{ba_2} - \frac{1}{2}(p\sqrt{r_1 r_2} + p'\sqrt{\gamma'_1 \gamma'_2}) \tilde{\rho}_{ba_1} + i[\Omega_2^*(2\rho_{a_2 a_2} + \rho_{a_1 a_1} + \rho_{cc} - 1) + \Omega_1^* \rho_{a_1 a_2}], \\
 \dot{\tilde{\rho}}_{ba_1} &= \left[ -\frac{1}{2}(r_1 + \gamma'_1) + i\Delta_1 \right] \tilde{\rho}_{ba_1} - \frac{1}{2}(p\sqrt{r_1 r_2} + p'\sqrt{\gamma'_1 \gamma'_2}) \tilde{\rho}_{ba_2} + i[\Omega_1^*(2\rho_{a_1 a_1} + \rho_{a_2 a_2} + \rho_{cc} - 1) + \Omega_2^* \rho_{a_2 a_1}], \\
 \dot{\tilde{\rho}}_{bc} &= \left[ -\frac{1}{2}(r_1 + r_2 + \gamma_0 + \gamma_1 + \gamma_2) + i(\Delta_1 + \delta_1) \right] \tilde{\rho}_{bc} + i(\Omega_2^* \tilde{\rho}_{a_2 c} + \Omega_1^* \tilde{\rho}_{a_1 c}), \\
 \dot{\rho}_{a_2 a_2} &= -(r_2 + \gamma'_2)\rho_{a_2 a_2} + (r_2 + \gamma_2)\rho_{cc} - \frac{1}{2}(p\sqrt{r_1 r_2} + p'\sqrt{\gamma'_1 \gamma'_2})(\rho_{a_2 a_1} + \rho_{a_1 a_2}) + i(\Omega_2 \tilde{\rho}_{ba_2} - \Omega_2^* \tilde{\rho}_{a_2 b}), \\
 \dot{\rho}_{a_2 a_1} &= \left[ -\frac{1}{2}(r_1 + r_2 + \gamma'_1 + \gamma'_2) - i(\Delta_2 - \Delta_1) \right] \rho_{a_2 a_1} - \frac{1}{2}(p\sqrt{r_1 r_2} + p'\sqrt{\gamma'_1 \gamma'_2})(\rho_{a_2 a_2} + \rho_{a_1 a_1}) \\
 &\quad + p\sqrt{r_1 r_2} \rho_{cc} + i(\Omega_2 \tilde{\rho}_{ba_1} - \Omega_1^* \tilde{\rho}_{a_2 b}), \\
 \dot{\tilde{\rho}}_{a_2 c} &= \left[ -\frac{1}{2}(r_1 + 2r_2 + \gamma_0 + \gamma_1 + \gamma_2 + \gamma'_2) + i\delta_2 \right] \tilde{\rho}_{a_2 c} - \frac{1}{2}(p\sqrt{r_1 r_2} + p'\sqrt{\gamma'_1 \gamma'_2}) \tilde{\rho}_{a_1 c} + i\Omega_2 \tilde{\rho}_{bc}, \\
 \dot{\rho}_{a_1 a_1} &= -(r_1 + \gamma'_1)\rho_{a_1 a_1} + (r_1 + \gamma_1)\rho_{cc} - \frac{1}{2}(p\sqrt{r_1 r_2} + p'\sqrt{\gamma'_1 \gamma'_2})(\rho_{a_2 a_1} + \rho_{a_1 a_2}) + i(\Omega_1 \tilde{\rho}_{ba_1} - \Omega_1^* \tilde{\rho}_{a_1 b}), \\
 \dot{\tilde{\rho}}_{a_1 c} &= \left[ -\frac{1}{2}(r_2 + 2r_1 + \gamma_0 + \gamma_1 + \gamma_2 + \gamma'_1) + i\delta_1 \right] \tilde{\rho}_{a_1 c} - \frac{1}{2}(p\sqrt{r_1 r_2} + p'\sqrt{\gamma'_1 \gamma'_2}) \tilde{\rho}_{a_2 c} + i\Omega_1 \tilde{\rho}_{bc}, \\
 \dot{\rho}_{cc} &= -(r_1 + r_2 + \gamma_0 + \gamma_1 + \gamma_2)\rho_{cc} + r_1 \rho_{a_1 a_1} + r_2 \rho_{a_2 a_2} + p\sqrt{r_1 r_2}(\rho_{a_1 a_2} + \rho_{a_2 a_1}). \tag{9}
 \end{aligned}$$

Here, we have introduced parameters  $p$  and  $p'$  to incorporate the fact that the dipole moments for the corresponding transitions may not be exactly parallel to each other. For example,  $p=1$  and  $p=0$  correspond to the case of dipole moments of the transitions  $|a_2\rangle \rightarrow |c\rangle$  and  $|a_1\rangle \rightarrow |c\rangle$  being parallel and perpendicular, respectively. Similarly  $p'$  corresponds to the transitions from  $|a_2\rangle$ ,  $|a_1\rangle$  to  $|b\rangle$ . Thus, these parameters are the measure of the relative orientation of the corresponding dipole moments. The actual form of them is given later. For most part, we use the values of  $p$  and  $p'$  from the set of  $\{0,1\}$  corresponding to the extremes of parallel and orthogonal dipole moments to study the effect of the absence or the presence of the interference terms on the behavior of the system. The detunings,  $\Delta_1 = \omega_{a_1 b} - \nu$ ,  $\Delta_2 = \omega_{a_2 b} - \nu$ ,  $\delta_1 = \omega_{ca_1} - \nu_p$ , and  $\delta_2 = \omega_{ca_2} - \nu_p$  appear in the above equations as we are in the rotated frames defined by

$$\rho = e^{-i\nu t} e^{-i\nu_p t} \tilde{\rho}, \tag{10}$$

where  $\nu$  and  $\nu_p$  are the frequencies of the coherent and in-

coherent fields, respectively. It will be apparent later that the interference of the two incoherent pump processes and the two decay processes among themselves are very important for quenching of spontaneous emission and is governed by the  $\sqrt{r_1 r_2}$  and the  $\sqrt{\gamma'_1 \gamma'_2}$  terms in the density-matrix equations, respectively.

### III. DRESSED-STATE ANALYSIS

Although, the interference terms can be clearly seen in the density-matrix equations (9) they still have a formidable appearance. It is very difficult to extract useful physical insight about the system from such a set of coupled equations even in steady state. However, atom-field combined dressed states provide a useful tool to acquire physical insight in such a complicated multilevel atomic system interacting with various electromagnetic fields and/or a reservoir [16]. In the current situation, it is instructive to dress the atom with the coherent field and see the effect and interaction of the vacuum and pumpings fields on such dressed states. In this

section, we first determine the form of the dressed states and then consider the effect of the vacuum and pumping interactions in the dressed-state picture.

### A. Determination of the combined atom-field dressed states

We start with defining the atom-field combined dressed states for the system. To incorporate the coherent light field in the state representation, we quantize it and resort to the number state representation of the same. The effect of the free energies and the coherent coupling can be summarized through the existence of the dressed states obtained by diagonalizing the corresponding Hamiltonian. For simplicity, we consider a slightly different representation for the Hamiltonian than the one considered in previous sections.

The atom-field combined states for the model of Fig. 1 can be taken to be  $|a_1, n\rangle$ ,  $|a_2, n\rangle$ ,  $|b, n\rangle$ , and  $|c, n\rangle$  where  $n$  denotes the number of photons in the coherent-field coupling state  $|b\rangle$  to  $|a_1\rangle$  and  $|a_2\rangle$ . The atom-field dressed states are just the eigenstates of the coherent-field coupling part of the Hamiltonian, namely,  $\mathcal{V}_1$ . To start with, we rewrite  $\mathcal{V}_1$  and the free-energy part of Hamiltonian in the interaction picture as

$$\begin{aligned} \mathcal{V} = & \hbar \Delta_1 |b\rangle \langle b| + \hbar \Delta_2 |a_2\rangle \langle a_2| - (\hbar g_1 |a_1\rangle \langle b| + \hbar g_2 |a_2\rangle \\ & \times \langle b| + \text{H.c.}), \end{aligned} \quad (11)$$

where  $g_{1,2}$  are the coupling constants between  $|a_{1,2}\rangle$  and  $|b\rangle$ . Here, we have also introduced the annihilation and creation operators denoted by  $a$  and  $a^\dagger$ , respectively, to achieve the quantized description of the coherent field. The corresponding characteristic equation is

$$\begin{aligned} \lambda_n^3 - \lambda_n^2(\Delta_1 + \Delta_2) - \lambda_n[g_1^2(n+1) + g_2^2(n+1) - \Delta_1\Delta_2] \\ + \Delta_1 g_2^2(n+1) + \Delta_2 g_1^2(n+1) = 0. \end{aligned} \quad (12)$$

For simplicity, we assume that

$$\Delta_1 g_2^2 + \Delta_2 g_1^2 = 0, \quad (13)$$

leading to a trivial solution  $\lambda_n^{(0)} = 0$  for the eigenvalue. The corresponding eigenstate is

$$\begin{aligned} |0, n\rangle = N_{0,n} \left[ g_2 \sqrt{n+1} |a_1, n\rangle - g_1 \sqrt{n+1} |a_2, n\rangle \right. \\ \left. - \frac{g_2}{g_1} \Delta_1 |b, n+1\rangle \right]. \end{aligned} \quad (14)$$

The other eigenstates can be shown to be

$$\begin{aligned} |\pm, n\rangle = N_{\pm, n} \left[ g_1 \sqrt{n+1} \left( \mu \pm \frac{\omega_{12}}{2} \right) |a_1, n\rangle \right. \\ \left. + g_2 \sqrt{n+1} \left( \mu \mp \frac{\omega_{12}}{2} \right) |a_2, n\rangle \right. \\ \left. \pm (g_1^2 + g_2^2)(n+1) |b, n+1\rangle \right], \end{aligned} \quad (15)$$

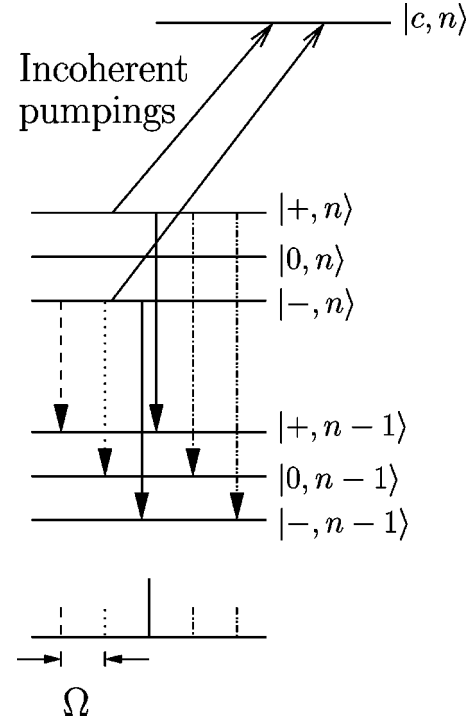


FIG. 2. Dressed-state representation of the level scheme. A typical spectrum is shown at the bottom of the figure, along with the corresponding spontaneous transitions introduced by the interaction with the vacuum field. Incoherent pumpings couple dressed states to the state  $|c, n\rangle$  as discussed in the text.

where  $N_{0,n}$  and  $N_{\pm, n}$  are the normalization constants and

$$\mu = \sqrt{g_1^2(n+1) + g_2^2(n+1) + \frac{\omega_{12}^2}{4}}, \quad (16)$$

with  $\omega_{12} = \omega_{a_1 b} - \omega_{a_2 b}$  being the spacing between the two upper levels. The corresponding eigenvalues are

$$\lambda_n^{(\pm)} = \frac{\Delta_1 + \Delta_2}{2} \pm \mu. \quad (17)$$

In Fig. 2, we show a set of two eigenstates differing in the photon number by one, thus, they differ in their energy by  $\hbar \nu$  corresponding to the energy carried by single photon.

The figure also shows that the adjacent set of dressed states couple with each other through spontaneous transitions and a given set of states couples to the state  $|c, n\rangle$  through the incoherent pumpings. However, only some of these couplings are possible and some are forbidden. We discuss these details in forthcoming sections.

### B. Coupled decay channels and dressed-state transitions

The decays from the upper-level doublet to the ground level in the bare basis amount to decays between two sets of the dressed states differing in the photon number by one. As discussed above the interaction Hamiltonian for these transitions is given by

$$\begin{aligned} \mathcal{V}_{\text{vacuum}} = & -\hbar \sum_k g_k^{(1)} e^{-i\nu_k t} |a_1\rangle \langle b| \hat{b}_k \\ & + g_k^{(2)} e^{-i\nu_k t} |a_2\rangle \langle b| \hat{b}_k + \text{H.c.}, \end{aligned} \quad (18)$$

where  $\nu_k$  corresponds to the frequency of the  $k$ th mode of emitted field. It can be shown that the decay interaction introduces transitions among the dressed states associated with different number of photons. For example, the matrix element for the transition from the dressed state  $|\pm, n+1\rangle$  to the state  $|0, n\rangle$  can be written as

$$\begin{aligned} V_{0,\pm,n}(t) = & \langle 0, n | \langle 1_k | \mathcal{V}_{\text{vacuum}} | \pm, n+1 \rangle | \{0\} \rangle \\ = & N_{0,n} N_{\pm,n+1} \langle 0, n | [ \hbar g_k^{(1)} g_1 \sqrt{n+2} \mu_1 \hbar g_k^{(2)} g_2 \\ & \times \sqrt{n+2} \mu_2 ] e^{i(\nu_k - \nu_0)t} | b, n+1 \rangle \\ = & N_{0,n} N_{\pm,n+1} \left( -\frac{g_2}{g_1} \Delta_1 \right) [ \hbar g_k^{(1)} g_1 \sqrt{n+2} \mu_1 \\ & + \hbar g_k^{(2)} g_2 \sqrt{n+2} \mu_2 ] e^{i(\nu_k - \nu_0)t}, \end{aligned} \quad (19)$$

where  $\mu_1 = \mu \pm \omega_{12}/2$  and  $\mu_2 = \mu \mp \omega_{12}/2$ . On the other hand, matrix elements of elements of the transitions from  $|0, n+1\rangle$  to  $|\pm, n\rangle$  are given by

$$\begin{aligned} V_{\pm,0,n}(t) = & \langle \pm, n | \langle 1_k | \mathcal{V}_{\text{vacuum}} | 0, n+1 \rangle | \{0\} \rangle = N_{\pm,n} N_{0,n+1} | \\ & \pm, 0 \rangle [ \hbar g_k^{(1)} g_2 \sqrt{n+2} \\ & - \hbar g_k^{(2)} g_1 \sqrt{n+2} ] e^{i(\nu_k - \nu_0)t} | b, n+1 \rangle \\ = & N_{\pm,n} N_{0,n+1} [ \pm (g_1^2 + g_2^2) (n+1) ] e^{i(\nu_k - \nu_0)t} \\ & \times [ \hbar g_k^{(1)} g_2 \sqrt{n+2} - \hbar g_k^{(2)} g_1 \sqrt{n+2} ]. \end{aligned} \quad (20)$$

It is clear that the matrix element (20) is zero when

$$\frac{g_k^{(1)}}{g_k^{(2)}} = \frac{g_1}{g_2} \quad (21)$$

for the arbitrary mode of the vacuum field. Since, by definition,

$$\frac{g_k^{(1)}}{g_k^{(2)}} = \frac{\vec{\mu}_{a_1,b} \cdot \hat{\mathbf{e}}_k}{\vec{\mu}_{a_2,b} \cdot \hat{\mathbf{e}}_k}, \quad (22)$$

where  $\hat{\mathbf{e}}_k$  is the unit vector of the  $k$ th radiation mode and  $\vec{\mu}_{a_j,b}$ 's are the matrix elements of the dipole moments of the two transitions, the parallel matrix elements of the two dipole moments are needed for vanishing  $V_{\pm,0,n}$  of Eq. (20) for arbitrary polarization of the vacuum field, assuming that  $g_1$  and  $g_2$  have the same sign. In the case when  $g_1$  and  $g_2$  have opposite signs, matrix element (20) will be zero for each vacuum mode, if the dipole moments are antiparallel.

Thus, we can have no decay from  $|0, n+1\rangle$  to  $|\pm, n\rangle$  under the condition (21). On the other hand, under the same condition the matrix element (19) is maximal, and the decay rates from  $|\pm, n+1\rangle$  to the  $|0, n\rangle$  do not vanish. Therefore,

under the above condition, the dressed states  $|\pm\rangle$  can decay into the dressed state  $|0\rangle$ , but not vice versa. The condition (21) can be rewritten as

$$\frac{g_1}{g_2} = p' \sqrt{\frac{\gamma'_1}{\gamma'_2}}, \quad (23)$$

where we have expressed  $g_k^{(1)}$  and  $g_k^{(2)}$  in terms of the corresponding radiative decay rates,  $\gamma'_1$  and  $\gamma'_2$ , as defined in the Appendix A and  $p'$  is the alignment of the dipole moments corresponding to the driven transitions,

$$p' = \frac{\vec{\mu}_{a_1,b} \cdot \vec{\mu}_{a_2,b}}{|\vec{\mu}_{a_1,b}| |\vec{\mu}_{a_2,b}|}. \quad (24)$$

With the introduction of the Rabi frequencies  $\Omega_{1,2} = g_{1,2} \sqrt{n+1}$  the trapping condition becomes

$$\frac{\Omega_1}{\Omega_2} = p' \sqrt{\frac{\gamma'_1}{\gamma'_2}}. \quad (25)$$

The Fig. 2 takes into account these selection rules when the trapping condition (25) is satisfied and gives a typical spontaneous emission spectrum with appropriate relative heights of the peaks. It, however, does not include the influence of the incoherent pumpings on the spectrum.

### C. Dressed states and incoherent pumping fields

The incoherent pumping interaction

$$\mathcal{V}_3 = -p_1 \mathcal{E}_p |c\rangle \langle a_1| - p_2 \mathcal{E}_p |c\rangle \langle a_2| + \text{H.c.} \quad (26)$$

ouples the dressed states to state  $|c, n\rangle$ . Matrix element of the incoherent pumping interaction between state  $|0, n\rangle$  and the state  $|c, n\rangle$  can be shown to be

$$\begin{aligned} V_{c,0;n} = & \langle c, n | \langle \{0\} | \mathcal{V}_3 | 0, n \rangle | \{0\} \rangle \\ = & N_{0,n} [ \hbar g_2 \sqrt{n+1} p_1 \mathcal{E}_p - \hbar g_1 \sqrt{n+1} p_2 \mathcal{E}_p ]. \end{aligned} \quad (27)$$

We can see that this matrix element vanishes if

$$\frac{p_1}{p_2} = p \sqrt{\frac{r_1}{r_2}} = \frac{g_1}{g_2} = \frac{\Omega_1}{\Omega_2}. \quad (28)$$

Here, we have expressed  $p_1$  and  $p_2$  in terms of the corresponding pumping rates,  $r_1$  and  $r_2$ , as defined in the Appendix B. Moreover,  $p$  corresponds to the relative orientations of the corresponding dipole moments

$$p = \frac{\vec{\mu}_{a_1,c} \cdot \vec{\mu}_{a_2,c}}{|\vec{\mu}_{a_1,c}| |\vec{\mu}_{a_2,c}|}. \quad (29)$$

Under the condition (28) it can be easily verified that the other matrix element corresponding to transition from state  $|\pm, n\rangle$  to state  $|c, n\rangle$  does not vanish. Thus, there are certain



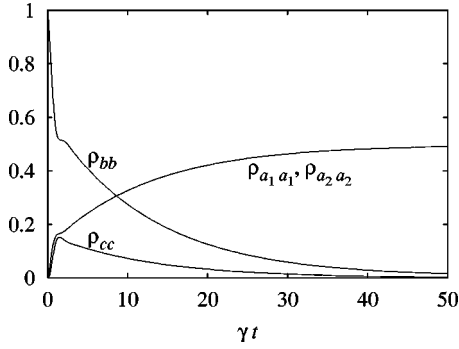


FIG. 3. Time evolution of populations for  $\omega_{a_2 a_1} = 0.2\gamma$ ,  $\Delta_1 = \delta_2 = -\Delta_2 = -\delta_1 = 0.1\gamma$ ,  $\Omega_1 = \Omega_2 = \gamma$ ,  $\gamma_1 = \gamma_2 = \gamma_0 = 0.5\gamma$ , and  $\gamma'_1 = \gamma'_2 = \gamma$ .

selection rules for transitions from the dressed states to the state  $|c, n\rangle$ , provided the trapping conditions are satisfied.

The dressed-state picture gives a good physical idea of the effect of the pumpings and vacuum coupling on the system as discussed above. However, a complete analysis of the system in the dressed-state picture could get extremely complicated. Therefore, to clarify these effects further, we study the complete numerical solution and so obtained results in the following section.

#### IV. RESULTS AND DISCUSSION

The set of density-matrix equations (9) can be easily solved to obtain the time evolution of populations and coherences as well as their steady-state behavior. The parameters chosen in all the figures satisfy the trapping conditions (25) and (28).

We summarize a typical result in Fig. 3 for the time dependence of the populations for all the four states. We start with all the population in state  $|b\rangle$  at time  $t=0$ , and it all ends up in states  $|a_1\rangle$  and  $|a_2\rangle$  in the steady state. Some of it is transferred to state  $|c\rangle$  because of the presence of the drive and the pump fields but it soon decays and we get almost 100% trapping in states  $|a_1\rangle$  and  $|a_2\rangle$ . Thus, we observe that there is a possibility of trapping all the population in states  $|a_1\rangle$  and  $|a_2\rangle$  even in the presence of apparent loss mecha-

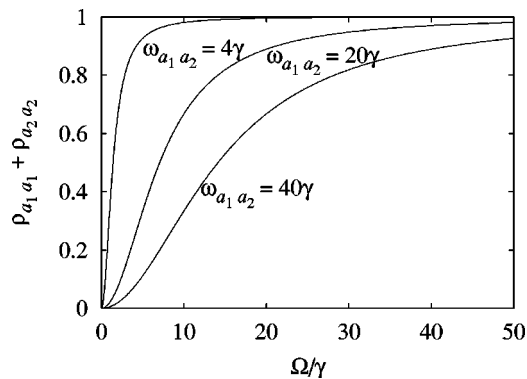


FIG. 4. Populations of the trapping states versus Rabi frequency.  $r_1 = r_2 = \gamma$ ,  $\Delta_1 = -\Delta_2 = -\delta_1 = \delta_2 = 0.5\omega_{a_2 a_1}$ , and  $\gamma_1 = \gamma_2 = \gamma_0 = \gamma'_1 = \gamma'_2 = \gamma$ .

nisms like the decays to state  $|b\rangle$  and pumpings to state  $|c\rangle$ . Once such coherent population trapping is achieved there is no spontaneous emission from the system.

Another important observation is the dependence of the amount of trapping on the energy spacing between the states  $|a_1\rangle$  and  $|a_2\rangle$ . We observe that the amount of trapping decreases with the increase in the energy spacing between the states  $|a_1\rangle$  and  $|a_2\rangle$ . Although, there is a possibility of increasing the Rabi frequency of the driving field in order to increase the trapped fraction. This is depicted in Fig. 4, where we plot the populations of the two upper-levels as a function of the Rabi frequency for different upper-level separations. Larger upper level separation needs larger Rabi frequency for the driving field to achieve the same fraction of population in the trapping states.

We now discuss the importance of the incoherent pumpings and the interference terms between them as well as the interference between the decay channels. We carefully study the effect of these terms on the population trapping in the doublet  $|a_1\rangle$  and  $|a_2\rangle$  for various relative values of the pumping and the decay parameters, while keeping all the other parameters fixed. The results are summarized in Fig. 5. We observe that the process of generating coherence between the decaying doublet through interference of incoherent pumpings is effective when the pumping parameters ( $r_1, r_2$ ) are at least three orders of magnitude larger than the decay parameters ( $\gamma'_1, \gamma'_2$ ). In this case, we observe that even in the absence of interference between the decay channels there is near 100% trapping and, thus, almost complete spontaneous emission quenching in the steady state.

This situation is particularly of interest as it implies that one can achieve tremendous control over the spontaneous emission from the decaying doublet even in the absence of the interference between the decay channels. In real life situations one does not have any control over the spontaneous decay properties of the atomic system let alone ensuring the presence of interference between two decay channels in order to quench the spontaneous emission. The first plot of Fig. 5 clearly illustrates that our model removes this stringent requirement on the decay properties of the system and imparts an easily controllable handle through the incoherent pumping parameters. Thus it could be easily implemented experimentally.

Observing part 2 and 3 of Fig. 5 illustrates that the above mentioned advantage is lost when the pumping parameters become comparable to or smaller than the decay parameters. When the pumping parameter values are comparable to those of the decay parameters the results obtained in the case of absence of either of the interference term are very close to each other as expected. However, a point to be noted is that still the precedence taken by the pump interference over the decay interference is clear in part 2 of Fig. 5. In the case where the pumpings are small compared to the decay parameters (part 3), we observe a role reversal and the influence of decay interference is larger compared to the pump interference as can be expected. Nevertheless, in all the cases when both the interference terms are present in the system, we have 100% trapping and complete spontaneous emission quenching.

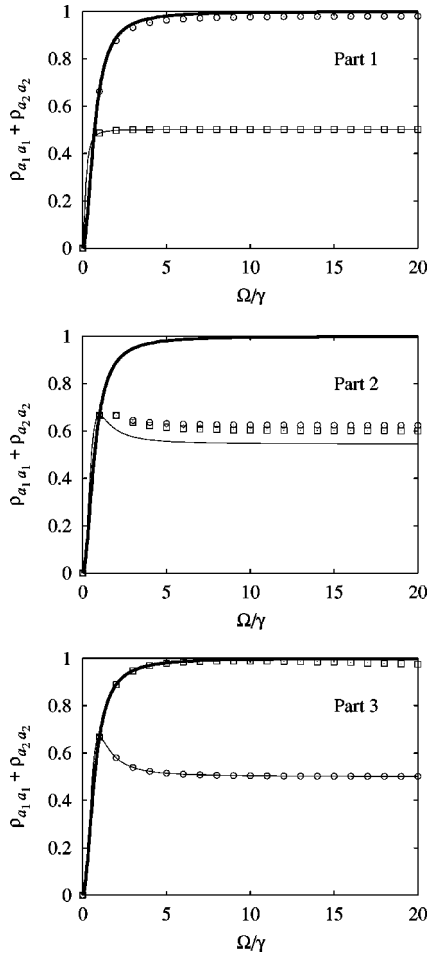


FIG. 5. Amount of trapping ( $\rho_{a_1 a_1} + \rho_{a_2 a_2}$ ) versus Rabi frequency  $\Omega/\gamma$  of the coherent field. In all the three parts of the figure thin line corresponds to case  $p=0, p'=0$ , i.e., the absence of both the interference terms; squares for  $p=0, p'=1$ , i.e., the presence of interference in the decay channels only; circles for  $p=1, p'=0$ , i.e., interference in the pumpings only; and thick line for  $p=1, p'=1$ , i.e., the presence of both the interference terms. The common parameters are the level spacing  $\omega_{a_1 a_2} = 2\gamma$ , other decay rates  $\gamma_1 = \gamma_2 = \gamma_0 = 0.1\gamma$ , and the decay rates of interest  $\gamma'_1 = \gamma'_2 = 0.001\gamma$ . Part 1 corresponds to the case of large pumping parameters compared to the decay parameters, i.e.,  $r_1 = r_2 = 10\gamma$ . Here, we observe that in the absence of both the interference terms, there is only 50% trapping as one would expect. However, the highlight is that even in the absence of interference in the decay channels there is near 100% trapping. Part 2 corresponds to  $r_1 = r_2 = \gamma'_1 = \gamma'_2 = 0.001\gamma$ . In this case, the results for the the case of either interference term being absent are close to each other. Other results are similar to the ones in part 1. It is clear that the effect of interference due to the incoherent pumpings is little more compared to the same due to the decay channels. Part 3, here, the pumping parameters are much smaller compared to the decay parameters, i.e.,  $r_1 = r_2 = 10^{-7}\gamma$ , and we observe a role reversal among the two interference terms. Thus, there is a swapping between the circles and squares compared to the corresponding case of part 1.

In Fig. 6, we plot the spontaneous emission spectrum of radiation emitted by the transitions  $|a_1\rangle \rightarrow |b\rangle$  and  $|a_2\rangle \rightarrow |b\rangle$ . The details of the spectrum calculations are given in Appendix C. As we can see it is a spectrum with five peaks

within the vicinity of the frequency of the driving field; the number of peaks can be easily explained in the dressed-state picture.

The total spontaneous emission in all the modes from states  $|a_1\rangle$  and  $|a_2\rangle$  is governed by the area under the spectral curve. We can easily see that the presence or absence of the interference terms in the decay and pump channels is of utmost importance in governing the total emission from the atom in the two decay channels. The presence of both the interference between the pump processes ( $p=1$ ) and decay processes ( $p'=1$ ) gives the spectrum with almost zero area under the curve. Thus, one can achieve complete spontaneous emission quenching.

## V. REVIEW OF THE MODEL CONSIDERED IN REF. [7] AND ITS COMPARISON WITH THE PRESENT ONE

So far, we have discussed the present model in its complete details and we have discussed the results in preceding section. It is more instructive to compare the results obtained here with a model previously considered in the literature to throw more light on the problem of spontaneous emission control and manipulation.

A scheme considered Ref. [7] is particularly of interest, due to its similarity to the current model. The system consists of a four-level atom very similar to the one considered here and is depicted in Fig. 7. Leaving aside the incoherent pumpings in this model, as there are no interference terms associated with them, the essential elements consist of a coherent field and interfering decay channels. Unlike the current model, this model achieves coherence between the decaying doublet through a coherent-field coupling with an outside level which has to lie below the doublet. Thus, a typical spontaneous emission spectrum consists of three distinct peaks as opposed to five in the present model. Another essential ingredient is the interference required among the decays from levels  $|a_1\rangle$  and  $|a_2\rangle$  to level  $|b\rangle$ .

The presence of the coherent field assures that the decaying doublet does not have to lie very close to each other. This aspect is essentially the same as in our model. Since the level  $|b\rangle$  in the model of Fig. 7 is lying lower than the decaying doublet there is extra set of spontaneous decay channels. It is shown in Ref. [7] interference is required on these decay channels too. This conditions is fairly stringent and can be very difficult to meet in real life situations.

The model of this paper (Fig. 1), does not impose any stringent requirements. Our results even relax the requirement of interference among the decay channels by choosing appropriate values for the pumping parameters. Achieving interference in the incoherent pumping is fairly easy experimentally by tweaking the polarization of the applied light field. Moreover, we observe that one can obtain more control over the spontaneous emission through the present scheme. Under similar conditions one obtains much less emission in all the modes in the present scheme compared to the one in Fig. 7. Thus, the present scheme can be more easily employed in experimental situations and gives more control over the amount of spontaneous emission from the system.

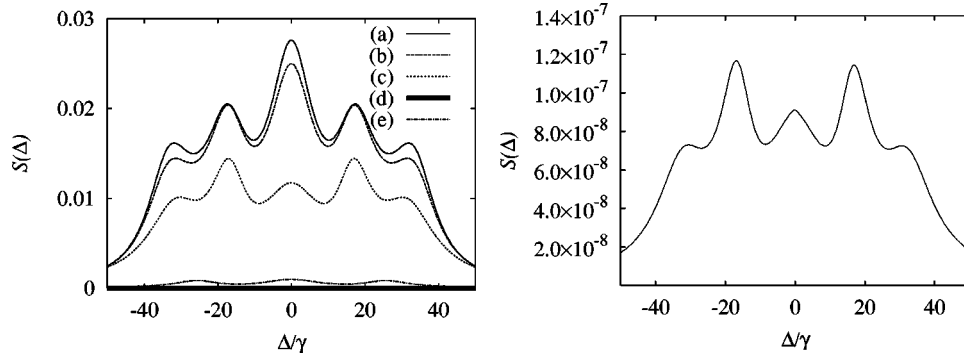


FIG. 6. Spontaneous emission spectrum. Parameter values for plots (a)–(d);  $\omega_{a_2 a_1} = 20\gamma$ ,  $\gamma'_1 = \gamma'_2 = \gamma_1 = \gamma_2 = \gamma_0 = \gamma$ ,  $\Omega_1 = \Omega_2 = 10\gamma$ ,  $r_1 = r_2 = 10\gamma$ . Left: Spontaneous emission spectrum for four different cases of the values of  $p$  and  $p'$  corresponding to the parallel and perpendicular directions of the corresponding dipole moments. The four different cases possible are depicted in (a)  $p = p' = 0$ , (b)  $p = 0$ ,  $p' = 1$ , (c)  $p = 1$ ,  $p' = 0$ , and (d)  $p = p' = 1$ . Plot (e) corresponds to the parameter values of Part 1 of Fig. 5 with  $p = 1$ ,  $p' = 0$ . Observe that in this scale the case (d) lies on the zero line. Moreover, in the case (e) is very close to the zero line illustrating the control one can achieve over spontaneous emission even in the absence of coupling in the decay channels. Right: The magnification of the zero line in the left part of the figure. The shape of the spectrum is preserved but the emission is negligible. Here,  $\Delta = (\omega - \nu)$  in the units of  $\gamma$ .

## VI. CONCLUSIONS

We have shown that atomic coherence can be generated through the interference of incoherent pump processes. This imparts an easily controllable handle for manipulating the spontaneous emission properties of three-level V-type system. Whereas, the interference between the decay channels is essential for complete quenching of spontaneous emission, the nature does not give us any control over the characteristic decays of any given system. In such a situation, being able to modify the coherence through the interference of external pumping fields, offers more control in achieving the right amount of trapping and fluorescence as needed. We have also shown that, under certain conditions, complete spontaneous emission quenching is possible in all the modes of the radiation field. We have also shown that with a certain choice of parameters it is possible to obtain near 100% trapping and almost complete quenching of spontaneous emission from a doublet even without the stringent requirement of the existence of interference in the decay channels. Our scheme can be very easily implemented experimentally as it works around the difficulty of finding the right kind of system with interfering decay channels.

## ACKNOWLEDGMENTS

The authors gratefully acknowledge the support from Air Force Research Laboratories (Rome, New York), DARPA-

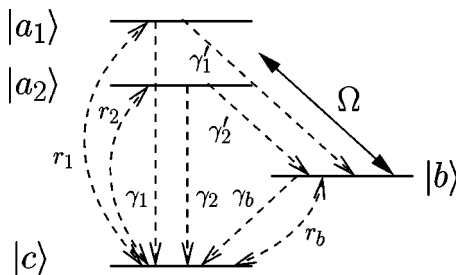


FIG. 7. Level scheme of Ref. [7].

QuIST, TAMU Telecommunications and Informatics Task Force (TITF) Initiative, and the Robert Welch Foundation.

## APPENDIX A: INTERFERENCE TERM FOR THE DECAY CHANNELS

We discuss the effect of  $\mathcal{V}_2$  on the density-matrix elements in this appendix. We consider all the four levels without the presence of the pumping terms and decays from state  $|c\rangle$  to  $|a_1\rangle$  and  $|a_2\rangle$ . Even though there is no direct coupling to state  $|c\rangle$ , as it will be evident later some coherence terms involving state  $|c\rangle$  are still present and do get affected by the interference of the decay processes.

The coupling of the atomic system to the vacuum reservoir is described through

$$\mathcal{V}_2 = -\hbar \sum_k g_k^{(1)} e^{-i\nu_k t} |a_1\rangle \langle b| \hat{b}_k + g_k^{(2)} e^{-i\nu_k t} |a_2\rangle \langle b| \hat{b}_k + \text{H.c.}, \quad (\text{A1})$$

as mentioned earlier. The Liouville equation for the total density operator  $\rho_T$  of the “atom + reservoir” system in the interaction representation is

$$\dot{\rho}_T = -\frac{i}{\hbar} [V_2(t), \rho_T(t)]. \quad (\text{A2})$$

Integrating the above equation once and substituting the result in it, we obtain

$$\begin{aligned} \dot{\rho}_T = & -\frac{i}{\hbar} [V_2(t), \rho_T(0)] \\ & + \left( \frac{i}{\hbar^2} \right) \int_0^t dt' [V_2(t), [V_2(t'), \rho_T(t')]], \end{aligned} \quad (\text{A3})$$

with the initial conditions given by

$$\rho_T(0) = \rho^{(2)}(0) \rho_F, \quad \rho_F \equiv \langle \{0_k\} | | \{0_k\} \rangle, \quad (\text{A4})$$



where,  $\rho^{(2)}(0)$  denotes the atomic density operator at  $t=0$ ,  $\rho_F$  the field density operator, and  $\{|0_k\rangle\}$  corresponds to the vacuum state. We now assume, as usually done when the system of interest is weakly coupled to a large reservoir, that the total density operator factorizes into the form

$$\rho_T = \rho^{(2)}(t)\rho_F \quad (\text{A5})$$

for any  $t>0$ ; in addition, we calculate the partial trace of above equation over the field degrees of freedom. Thus, from straightforward calculations, it follows that the atomic density matrix element  $\rho_{ba_2}^{(2)}$  satisfies the equation of motion

$$\begin{aligned} \dot{\rho}_{ba_2}^{(2)} &= - \int_0^t dt' \sum_k g_k^{(1)2} \exp[-i\nu_k(t-t')] \rho_{ba_2}^{(2)}(t') \\ &= - \int_0^t dt' \sum_k g_k^{(1)} g_k^{(2)} \exp[-i\nu_k t + i\nu_k' t'] \rho_{ba_1}^{(2)}(t'). \end{aligned} \quad (\text{A6})$$

At this point, usually, it is assumed that  $\rho_{ba_2}^{(2)}(t)$  and  $\rho_{ba_1}^{(2)}(t')$  are slowly varying functions of time and, therefore,  $\rho^{(2)}(t')$  can be replaced by  $\rho^{(2)}(t)$ . The  $t'$  integration in above equation is then carried out. Here, we follow a different procedure. First, we replace the summation over  $k$  by an integral, i.e.,

$$\sum_k \dots \rightarrow \int_{-\infty}^{\infty} d\nu_k \mathcal{D}(\nu_k) \dots, \quad (\text{A7})$$

where

$$\mathcal{D}(\nu_k) = \frac{V\nu_k^2}{\pi^2 c^3} \quad (\text{A8})$$

represents the density of states. Here,  $V$  is the quantization volume. On interchanging the integrations over  $\nu_k$  and  $t'$ , we obtain

$$\begin{aligned} \dot{\rho}_{ba_2}^{(2)} &= - \int_0^t dt' \int_{-\infty}^{\infty} d\nu_k \mathcal{D}(\nu_k) g_k^{(1)} \{ g_k^{(1)} \rho_{ba_2}^{(2)}(t) \\ &\quad \times \exp[-i\nu_k(t-t')] + g_k^{(2)} \rho_{ba_1}^{(2)}(t') \exp(-i\nu_k t) \\ &\quad \times \exp(-i\nu_k' t') \}. \end{aligned} \quad (\text{A9})$$

Now, we assume that the states  $|a_1\rangle$  and  $|a_2\rangle$  are close to each other. Thus, the density of states  $\mathcal{D}(\nu_k)$  and the coupling constants  $g_k^{(1)}$  and  $g_k^{(2)}$  contribute significantly only around  $\nu_k = \omega$ . We can, therefore, replace  $\nu_k$  by  $\omega$  in the corresponding terms. Thus,

$$\begin{aligned} \dot{\rho}_{ba_2}^{(2)} &= - \mathcal{D}(\omega) g_\omega^{(1)} \int_0^t dt' \int_{-\infty}^{\infty} d\nu_k \{ g_k^{(1)} \rho_{ba_2}^{(2)}(t) \\ &\quad \times \exp[-i\nu_k(t-t')] + g_k^{(2)} \rho_{ba_1}^{(2)}(t') \exp(-i\nu_k t) \\ &\quad \times \exp(-i\nu_k' t') \}. \end{aligned} \quad (\text{A10})$$

On carrying out the integration, we obtain

$$\dot{\rho}_{ba_2}^{(2)} = - \frac{1}{2} \gamma_2' \rho_{ba_2}^{(2)} - \frac{1}{2} \sqrt{\gamma_1' \gamma_2'} \rho_{ba_1}^{(2)}, \quad (\text{A11})$$

where  $\gamma_1' = 2\pi \mathcal{D}(\omega) g_\omega^{(1)2}$ ,  $\gamma_2' = 2\pi \mathcal{D}(\omega) g_\omega^{(2)2}$ . Here, we have assumed both coupling constants to be positive. Similar calculations lead to the equations for the remaining independent matrix elements

$$\begin{aligned} \dot{\rho}_{ba_1}^{(2)} &= - \frac{1}{2} \gamma_1' \rho_{ba_1}^{(2)} - \frac{1}{2} \sqrt{\gamma_1' \gamma_2'} \rho_{ba_2}^{(2)}, \\ \dot{\rho}_{a_2 a_2}^{(2)} &= - \gamma_2' \rho_{a_2 a_2}^{(2)} - \frac{1}{2} \sqrt{\gamma_1' \gamma_2'} (\rho_{a_2 a_1}^{(2)} + \rho_{a_1 a_2}^{(2)}), \\ \dot{\rho}_{a_2 a_1}^{(2)} &= - \frac{1}{2} (\gamma_1' + \gamma_2') \rho_{a_2 a_1}^{(2)} - \frac{1}{2} \sqrt{\gamma_1' \gamma_2'} (\rho_{a_2 a_2}^{(2)} + \rho_{a_1 a_1}^{(2)}), \\ \dot{\rho}_{a_1 a_1}^{(2)} &= - \frac{1}{2} \gamma_1' \rho_{a_1 a_1}^{(2)} - \frac{1}{2} \sqrt{\gamma_1' \gamma_2'} (\rho_{a_2 a_1}^{(2)} + \rho_{a_1 a_2}^{(2)}), \\ \dot{\rho}_{a_2 c}^{(2)} &= - \frac{1}{2} \gamma_2' \rho_{a_2 c}^{(2)} - \frac{1}{2} \sqrt{\gamma_1' \gamma_2'} \rho_{a_1 c}^{(2)}, \\ \dot{\rho}_{a_1 a_1}^{(2)} &= - \gamma_1' \rho_{a_1 a_1}^{(2)} - \frac{1}{2} \sqrt{\gamma_1' \gamma_2'} (\rho_{a_2 a_1}^{(2)} + \rho_{a_1 a_2}^{(2)}), \\ \dot{\rho}_{a_1 c}^{(2)} &= - \frac{1}{2} \gamma_1' \rho_{a_1 c}^{(2)} - \frac{1}{2} \sqrt{\gamma_1' \gamma_2'} \rho_{a_2 c}^{(2)}. \end{aligned} \quad (\text{A12})$$

We note that the terms containing the product of  $\gamma_1'$  and  $\gamma_2'$  describe quantum interference effects which emerge from the radiative decay of the upper states to their common lower level. In particular, this interference term is responsible for establishing the coherence between states  $|a_1\rangle$  and  $|a_2\rangle$ . The coherences  $\rho_{a_2 c}^{(2)}$  and  $\rho_{a_1 c}^{(2)}$  are affected by these interference terms even in the absence of any direct coupling of  $|c\rangle$  to the remaining states.

## APPENDIX B: INTERFERENCE TERM FOR THE PUMP PROCESSES

In this appendix, we consider the detailed calculation of the pump processes described by the Hamiltonian

$$\mathcal{V}_3 = -p_1 \mathcal{E}_p |c\rangle \langle a_1| - p_2 \mathcal{E}_p |c\rangle \langle a_2| + \text{H.c.} \quad (\text{B1})$$

As discussed in Sec. II we assume a the two-time correlation of the applied electric field to be  $\delta$ -like, i.e.,

$$\langle \mathcal{E}_p^*(t) \mathcal{E}_p(t') \rangle = \Gamma_p \delta(t-t'). \quad (\text{B2})$$

The Liouville equation for the density-matrix corresponding to this part of the integration is

$$\dot{\rho}^{(3)} = - \frac{i}{\hbar} [\mathcal{V}_3, \rho^{(3)}] = - \frac{i}{\hbar} (\mathcal{V}_3 \rho^{(3)} - \rho^{(3)} \mathcal{V}_3). \quad (\text{B3})$$

Expanding the Liouville equation, we arrive at

$$\begin{aligned}
\dot{\rho}_{ba_2}^{(3)} &= -\frac{i}{\hbar} p_2 \mathcal{E}_p \rho_{bc}^{(3)}, \\
\dot{\rho}_{ba_1}^{(3)} &= -\frac{i}{\hbar} p_1 \mathcal{E}_p \rho_{bc}^{(3)}, \\
\dot{\rho}_{bc}^{(3)} &= -\frac{i}{\hbar} \mathcal{E}_p^* (p_1 \rho_{ba_1}^{(3)} + p_2 \rho_{ba_2}^{(3)}), \\
\dot{\rho}_{a_2 a_2}^{(3)} &= \frac{i}{\hbar} p_2 (\mathcal{E}_p^* \rho_{ca_2}^{(3)} - \mathcal{E}_p \rho_{a_2 c}^{(3)}), \\
\dot{\rho}_{a_2 a_1}^{(3)} &= \frac{i}{\hbar} (p_2 \mathcal{E}_p^* \rho_{ca_1}^{(3)} - p_1 \mathcal{E}_p \rho_{a_2 c}^{(3)}), \\
\dot{\rho}_{a_2 c}^{(3)} &= \frac{i}{\hbar} [p_2 \mathcal{E}_p^* (\rho_{cc}^{(3)} - \rho_{a_2 a_2}^{(3)}) - p_1 \mathcal{E}_p^* \rho_{a_2 a_1}^{(3)}], \\
\dot{\rho}_{a_1 a_1}^{(3)} &= \frac{i}{\hbar} p_1 (\mathcal{E}_p^* \rho_{ca_1}^{(3)} - \mathcal{E}_p \rho_{a_1 c}^{(3)}), \\
\dot{\rho}_{a_1 c}^{(3)} &= \frac{i}{\hbar} [p_1 \mathcal{E}_p^* (\rho_{cc}^{(3)} - \rho_{a_1 a_1}^{(3)}) - p_2 \mathcal{E}_p^* \rho_{a_1 a_2}^{(3)}], \\
\dot{\rho}_{cc}^{(3)} &= \frac{i}{\hbar} \{ \mathcal{E}_p (p_1 \rho_{a_1 c}^{(3)} + p_2 \rho_{a_2 c}^{(3)}) - \mathcal{E}_p^* (p_1 \rho_{ca_1}^{(3)} + p_2 \rho_{ca_2}^{(3)}) \},
\end{aligned} \tag{B4}$$

as a starting point. The strategy is to integrate all these equations once and then resubstitute the so obtained equations back into the above equation, much like the method applied in Appendix A. We consider the evaluation of density-matrix equation for element  $\rho_{ba_2}^{(3)}$  in complete details. We need expression for  $\rho_{bc}^{(3)}(t)$ , which after formal integration of  $\dot{\rho}_{bc}^{(3)}$  equation from above is

$$\rho_{bc}^{(3)}(t) = -\frac{i}{\hbar} \int_0^t d\tau \mathcal{E}_p^*(\tau) [p_1 \rho_{ba_1}^{(3)}(\tau) + p_2 \rho_{ba_2}^{(3)}(\tau)]. \tag{B5}$$

Substituting in the  $\dot{\rho}_{ba_2}^{(3)}$  equation, we obtain

$$\begin{aligned}
\dot{\rho}_{ba_2}^{(3)} &= + \left( \frac{i}{\hbar} \right)^2 p_2^2 \int_0^t d\tau \mathcal{E}_p(t) \mathcal{E}_p^*(\tau) \rho_{ba_2}^{(3)}(\tau) \\
&+ \left( \frac{i}{\hbar} \right)^2 p_1 p_2 \int_0^t d\tau \mathcal{E}_p(t) \mathcal{E}_p^*(\tau) \rho_{ba_1}^{(3)}(\tau). \tag{B6}
\end{aligned}$$

Thus, using the  $\delta$  correlation of the pumping fields, we arrive at

$$\dot{\rho}_{ba_2}^{(3)} = -\frac{1}{2} r_2 \rho_{ba_2}^{(3)} - \frac{1}{2} \sqrt{r_1 r_2} \rho_{ba_1}^{(3)}, \tag{B7}$$

where we have defined

$$r_{1,2} \equiv 2(p_{1,2}^2 / \hbar^2) \Gamma_p. \tag{B8}$$

Following similar steps for the remaining matrix elements, we obtain

$$\begin{aligned}
\dot{\rho}_{ba_1}^{(3)} &= -\frac{1}{2} r_1 \rho_{ba_1}^{(3)} - \frac{1}{2} \sqrt{r_1 r_2} \rho_{ba_2}^{(3)}, \\
\dot{\rho}_{bc}^{(3)} &= -\frac{1}{2} (r_1 + r_2) \rho_{bc}^{(3)}, \\
\dot{\rho}_{a_2 a_2}^{(3)} &= -r_2 \rho_{a_2 a_2}^{(3)} + r_2 \rho_{cc}^{(3)} - \frac{1}{2} \sqrt{r_1 r_2} (\rho_{a_2 a_1}^{(3)} + \rho_{a_1 a_2}^{(3)}), \\
\dot{\rho}_{a_2 a_1}^{(3)} &= -\frac{1}{2} (r_1 + r_2) \rho_{a_2 a_1}^{(3)} + \frac{1}{2} \sqrt{r_1 r_2} (2\rho_{cc}^{(3)} - \rho_{a_2 a_2}^{(3)} - \rho_{a_1 a_1}^{(3)}), \\
\dot{\rho}_{a_2 c}^{(3)} &= -r_2 \rho_{a_2 c}^{(3)} - \frac{1}{2} r_1 \rho_{a_2 c}^{(3)} - \frac{1}{2} \sqrt{r_1 r_2} \rho_{a_1 c}^{(3)}, \\
\dot{\rho}_{a_1 a_1}^{(3)} &= -r_1 \rho_{a_1 a_1}^{(3)} + r_1 \rho_{cc}^{(3)} - \frac{1}{2} \sqrt{r_1 r_2} (\rho_{a_2 a_1}^{(3)} + \rho_{a_1 a_2}^{(3)}), \\
\dot{\rho}_{a_1 c}^{(3)} &= -r_1 \rho_{a_1 c}^{(3)} - \frac{1}{2} r_2 \rho_{a_1 c}^{(3)} - \frac{1}{2} \sqrt{r_1 r_2} \rho_{a_2 c}^{(3)}, \\
\dot{\rho}_{cc}^{(3)} &= -(r_1 + r_2) \rho_{cc}^{(3)} + r_1 \rho_{a_1 a_1}^{(3)} + r_2 \rho_{a_2 a_2}^{(3)} \\
&+ \sqrt{r_1 r_2} (\rho_{a_2 a_1}^{(3)} + \rho_{a_1 a_2}^{(3)}).
\end{aligned} \tag{B9}$$

We note that the terms involving products of  $r_1$  and  $r_2$  correspond to interference between the pumping processes from two lower lying states  $|a_1\rangle$  and  $|a_2\rangle$  to upper lying states  $|c\rangle$ . In particular, this interference term affects the coherence between states  $|a_1\rangle$  and  $|a_2\rangle$ . Moreover, even in the absence of any direct coupling with state  $|b\rangle$ , coherences  $\rho_{ba_2}^{(3)}$ ,  $\rho_{ba_1}^{(3)}$ , and  $\rho_{bc}^{(3)}$  are influenced by the interference of pumpings from states  $|a_1\rangle$  and  $|a_2\rangle$  to state  $|c\rangle$ .

### APPENDIX C: CALCULATION OF THE SPONTANEOUS EMISSION SPECTRUM

Spontaneous emission spectrum can be calculated as a Fourier transform of the two-time correlation function of electric-field intensity, i.e.,

$$S(\omega) = \frac{1}{2\pi} \int_0^\infty d\tau e^{-i\omega\tau} \langle \vec{E}^{(-)}(\vec{r}, t + \tau) \cdot \vec{E}^{(+)}(\vec{r}, t) \rangle + \text{c.c.}, \tag{C1}$$

where  $\vec{E}^{(+)}(\vec{r}, t)$  [ $\vec{E}^{(-)}(\vec{r}, t)$ ] is the positive (negative) part of the electric field operator at time  $t$  and position  $\vec{r}$ . In the far-zone approximation this operator takes the form

$$\vec{E}^{(+)}(\vec{r}, t) = \vec{E}_0^{(+)}(\vec{r}, t) - \frac{\omega_0^2}{4\pi\epsilon_0 c^2 r} \hat{n} \cdot [\hat{n} \cdot \vec{P}^{(+)}(t - r/c)], \quad (\text{C2})$$

where  $\hat{n}$  is the unit vector in the direction of observation,  $\vec{P}^{(+)}$  is the positive part of the atomic polarization operator in the Heisenberg picture. We are interested in the spectrum of radiation emitted by the transitions  $|a_1\rangle \rightarrow |b\rangle$  and  $|a_2\rangle \rightarrow |b\rangle$ . In this case,  $\omega_0 = (\omega_{a_1 b} + \omega_{a_2 b})/2$  and

$$\begin{aligned} \vec{P}^{(-)}(t) &= \vec{\mu}_{a_1 b}(|a_1\rangle\langle b|)^H(t) + \vec{\mu}_{a_2 b}(|a_2\rangle\langle b|)^H(t), \\ \vec{P}^{(+)}(t) &= [\vec{P}^{(-)}(t)]^\dagger, \end{aligned} \quad (\text{C3})$$

where superscript  $H$  denotes that the operators are taken in the Heisenberg picture. We note that

$$p' = \frac{\vec{\mu}_{a_1 b} \cdot \vec{\mu}_{a_2 b}}{\mu_{a_1 b} \mu_{a_2 b}}, \quad (\text{C4})$$

denotes the alignment of the dipole moments of the two transitions. From Eqs. (C2) and (C3), it follows that the spontaneous emission spectrum is proportional to the Fourier transform of the atomic two-time correlation function

$$\Gamma^{(1)}(t, \tau) = \langle \vec{P}^{(-)}(t + \tau) \vec{P}^{(+)}(t) \rangle. \quad (\text{C5})$$

Calculation of Eq. (C5) involves a straightforward application of the quantum regression theorem [17]. This theorem states that if, for some operator  $\hat{O}_i$ ,

$$\langle \hat{O}_i(t + \tau) \rangle = \sum_j c_j(t, \tau) \langle \hat{O}_j(t) \rangle, \quad (\text{C6})$$

where  $\{\hat{O}_j\}$  is a complete set of system operators and  $c_j$ 's are  $c$ -number functions of time, then

$$\langle \hat{O}_i(t + \tau) \hat{O}_k(t) \rangle = \sum_j c_j(t, \tau) \langle \hat{O}_j(t) \hat{O}_k(t) \rangle. \quad (\text{C7})$$

The density-matrix elements can be arranged in a vector form

$$\begin{aligned} R &= (\rho_{ba_2} \ \rho_{ba_1} \ \rho_{bc} \ \rho_{a_2 b} \ \rho_{a_2 a_2} \ \rho_{a_2 a_1} \ \rho_{a_2 c} \ \rho_{a_1 b} \\ &\times \rho_{a_1 a_2} \ \rho_{a_1 a_1} \ \rho_{a_1 c} \ \rho_{cb} \ \rho_{ca_2} \ \rho_{ca_1} \ \rho_{cc})^T, \end{aligned} \quad (\text{C8})$$

thus allowing to rewrite the density-matrix equations of motion in the following matrix form:

$$\dot{R} = MR + B, \quad (\text{C9})$$

where  $B$  is an inhomogeneous part arising from elimination of  $\rho_{bb}$  by normalization condition  $\sum_{i=a_1, a_2, b, c} \rho_{ii} = 1$ . Explicit expressions for the matrix  $M$  and vector  $B$  are too bulky to be presented here. They can be easily obtained from Eq. (9). The formal solution of the system (C9) can be written as

$$R(t) = \exp[M(t - t_0)]R(0) + \int_{t_0}^t dt' \exp[M(t - t')]B, \quad (\text{C10})$$

and the steady-state solution reads

$$R(t = \infty) = -M^{-1}B. \quad (\text{C11})$$

The first step in the application of the regression theorem is to find the one-time expectation value of the atomic polarization operator. The expectation values calculated in Schrödinger and Heisenberg pictures coincide, therefore,

$$\begin{aligned} \langle \vec{P}^{(-)}(t + \tau) \rangle &= \vec{\mu}_{a_1 b} \langle (|a_1\rangle\langle b|)^H(t + \tau) \rangle \\ &\quad + \vec{\mu}_{a_2 b} \langle (|a_2\rangle\langle b|)^H(t + \tau) \rangle \\ &= \vec{\mu}_{a_1 b} \rho_{a_1 b}^S(t + \tau) + \vec{\mu}_{a_2 b} \rho_{a_2 b}^S(t + \tau) \\ &= \vec{\mu}_{a_1 b} \rho_{a_1 b} e^{\omega_{a_1 b}(t + \tau)} + \vec{\mu}_{a_2 b} \rho_{a_2 b} e^{\omega_{a_2 b}(t + \tau)}. \end{aligned} \quad (\text{C12})$$

Here, the superscripts  $H$  and  $S$  stand for the Heisenberg and Schrödinger picture, respectively. Now in order to evaluate Eq. (C5), we need to rewrite this expectation value in terms of the system operators  $(|i\rangle\langle j|)^H$  and carry out the replacement

$$\langle (|i\rangle\langle j|)^H(t) \rangle \rightarrow \langle (|i\rangle\langle j| \vec{P}^{(+)}(t))^H(t) \rangle. \quad (\text{C13})$$

Taking the Fourier transform of the result, in the limit  $t \rightarrow \infty$ , we find the spontaneous emission spectrum in the form [18]

$$S(\omega) = \text{Re} \Gamma^{(1)}(z) \Big|_{z=i\omega}, \quad (\text{C14})$$

where

$$\begin{aligned}
\hat{\Gamma}(z) = & \mu_{a_1 b}^2 \left( L_{21}(z_1)R_9(\infty) + L_{22}(z_1)R_{10}(\infty) + L_{23}(z_1)R_{11}(\infty) + \sum_{j=1}^{15} P_{2j}(z_1)B_j R_8(\infty) \right) \\
& + p \vec{\mu}_{a_1 b} \cdot \vec{\mu}_{a_2 b} \left( L_{21}(z_1)R_5(\infty) + L_{22}(z_1)R_6(\infty) + L_{23}(z_1)R_7(\infty) + \sum_{j=1}^{15} P_{2j}(z_1)B_j R_4(\infty) \right) \\
& + p \vec{\mu}_{a_2 b} \cdot \vec{\mu}_{b a_1} \left( L_{11}(z_1)R_9(\infty) + L_{12}(z_1)R_{10}(\infty) + L_{13}(z_1)R_{11}(\infty) + \sum_{j=1}^{15} P_{1j}(z_1)B_j R_8(\infty) \right) \\
& + \mu_{a_2 b}^2 \left( L_{11}(z_1)R_5(\infty) + L_{12}(z_1)R_6(\infty) + L_{13}(z_1)R_7(\infty) + \sum_{j=1}^{15} P_{1j}(z_1)B_j R_4(\infty) \right), \tag{C15}
\end{aligned}$$

with

$$L(z_1) = (z_1 I - M)^{-1}, \quad P(z_1) = M^{-1}(z_1 I - M)^{-1}. \tag{C16}$$

Here, we have used the definition

$$z_1 = z - i\omega_0 = i(\omega - \omega_0) = i(\omega - \nu) = i\Delta, \tag{C17}$$

with  $\nu$  being the frequency of the coherent-field tuned to the middle of the two levels  $|a_1\rangle$  and  $|a_2\rangle$ . Thus, using the recipe discussed in this appendix the spectrum can be calculated numerically for different parameter values.

- 
- [1] M.O. Scully, Phys. Rev. Lett. **55**, 2802 (1985); M.O. Scully and M.S. Zubairy, Phys. Rev. A **35**, 752 (1987).
- [2] O. Kocharovskaya and Ya.I. Khanin, Pis'ma Zh. Éksp. Teor. Fiz. **48**, 581 (1988) [JETP Lett. **48**, 630 (1988)]; S.E. Harris, Phys. Rev. Lett. **62**, 1033 (1989); P. Mandel and O. Kocharovskaya, Phys. Rev. A **47**, 5003 (1993).
- [3] D.A. Cardimona, M.G. Raymer, and C.R. Stroud, J. Phys. B **15**, 55 (1982); A. Imamoglu, Phys. Rev. A **40**, 2835 (1989).
- [4] M.O. Scully, S.Y. Zhu, and A. Gavrielides, Phys. Rev. Lett. **62**, 2813 (1989).
- [5] A. Imamoglu and S.E. Harris, Opt. Lett. **14**, 1344 (1989).
- [6] S.-Y. Zhu and M.O. Scully, Phys. Rev. Lett. **76**, 388 (1996).
- [7] H. Lee, P. Polynkin, M.O. Scully, and S.-Y. Zhu, Phys. Rev. A **55**, 4454 (1997).
- [8] D. Agassi, Phys. Rev. A **30**, 2449 (1984).
- [9] S.-Y. Zhu, L.M. Narducci, and M.O. Scully, Phys. Rev. A **52**, 4791 (1995).
- [10] M. Fleischhauer, C.H. Keitel, M.O. Scully and C. Su, Opt. Commun. **87**, 109 (1992).
- [11] O. Kocharovskaya, A.B. Matsko, and Y. Rostovtsev, Phys. Rev. A **65**, 013803 (2001).
- [12] Z. Ficek and S. Swain, J. Mod. Opt. **49**, 3 (2002).
- [13] H.-R. Xia, C.-Y. Ye, and S.-Y. Zhu, Phys. Rev. Lett. **77**, 1032 (1996).
- [14] L. Li, X. Wang, J. Yang, G. Lazarov, J. Qi, and A.M. Lyyra, Phys. Rev. Lett. **84**, 4016 (2000).
- [15] M.O. Scully, and M.S. Zubairy, *Quantum Optics* (Cambridge University Press, Cambridge, U.K., 1997), Chap. 8.
- [16] C. Cohen-Tanoudji and S. Reynaud, J. Phys. B **10**, 345 (1977); **10**, 365 (1977); **10**, 2311 (1977).
- [17] L. Onsager, Phys. Rev. **37**, 405 (1931); M. Lax, *ibid.* **129**, 2342 (1963).
- [18] L.M. Narducci, M.O. Scully, G.-L. Oppo, P. Ru, and J.R. Tredicce, Phys. Rev. A **42**, 1630 (1990).